

## Lymphoid Neogenesis in Rheumatoid Synovitis

Seisuke Takemura, Andrea Braun, Cynthia Crowson, Paul J. Kurtin, Robert H. Cofield, William M. O'Fallon, Jörg J. Goronzy and Cornelia M. Weyand

This information is current as  
of August 9, 2022.

*J Immunol* 2001; 167:1072-1080; ;  
doi: 10.4049/jimmunol.167.2.1072  
<http://www.jimmunol.org/content/167/2/1072>

**References** This article **cites 41 articles**, 16 of which you can access for free at:  
<http://www.jimmunol.org/content/167/2/1072.full#ref-list-1>

**Why *The JI*? Submit online.**

- **Rapid Reviews! 30 days\*** from submission to initial decision
- **No Triage!** Every submission reviewed by practicing scientists
- **Fast Publication!** 4 weeks from acceptance to publication

*\*average*

**Subscription** Information about subscribing to *The Journal of Immunology* is online at:  
<http://jimmunol.org/subscription>

**Permissions** Submit copyright permission requests at:  
<http://www.aai.org/About/Publications/JI/copyright.html>

**Email Alerts** Receive free email-alerts when new articles cite this article. Sign up at:  
<http://jimmunol.org/alerts>

# Lymphoid Neogenesis in Rheumatoid Synovitis<sup>1</sup>

Seisuke Takemura,<sup>2\*</sup> Andrea Braun,<sup>2\*</sup> Cynthia Crowson,<sup>‡</sup> Paul J. Kurtin,<sup>†</sup> Robert H. Cofield,<sup>§</sup> William M. O'Fallon,<sup>‡</sup> Jörg J. Goronzy,<sup>\*</sup> and Cornelia M. Weyand<sup>3\*</sup>

In rheumatoid arthritis (RA), tissue-infiltrating lymphocytes can be arranged in sophisticated organizations that resemble microstructures usually formed in secondary lymphoid organs. Molecular pathways and host risk factors involved in this process of lymphoid neogenesis remain to be defined. In a series of 64 synovial tissue biopsies, lymphoid follicles with germinal centers (GCs) were found in 23.4% of the patients. Follicular dendritic cells (FDCs) were exclusively present in tissues with GCs, suggesting that the recruitment or in situ maturation of FDCs is a critical factor for GC formation in the synovial membrane. Primary follicles were absent, emphasizing the role of Ag recognition in the generation of inflammation-associated lymphoid organogenesis. Multivariate logistic regression analysis of tissue cytokines and chemokines identified two parameters, in situ transcription of lymphotoxin (LT)- $\beta$  and of B lymphocyte chemoattractant (BLC; BLC/CXCL13), that were predictors for FDC recruitment and synovial GC formation. LT- $\beta$  and BLC/CXCL13 were found to be independent variables that could, in part, compensate for each other to facilitate GC formation. Prediction models incorporating in situ transcription of LT- $\beta$  and BLC/CXCL13 had high negative yet moderate positive predictive values, suggesting that LT- $\beta$  and BLC/CXCL13 are necessary but not sufficient. LT- $\beta$  protein was detected on a subset of mantle zone and GC B cells, but also on T cells in follicular structures. BLC/CXCL13 was produced by FDCs in follicular centers, but was predominantly found in endothelial cells and synovial fibroblasts, suggesting heterotypic signaling between cells of the synovial membrane and infiltrating lymphocytes in regulating extranodal lymphoid neogenesis. *The Journal of Immunology*, 2001, 167: 1072–1080.

The preferred targets of inflammatory attack in rheumatoid arthritis (RA)<sup>4</sup> are the synovial membrane, cartilage, and bone of diarthrodial joints. T cells, B cells, macrophages, and dendritic cells (DCs) accumulate in the synovial layer, inducing hyperplasia and tissue invasiveness of the synoviocytes. A distinguishing feature of the rheumatoid lesion is the high degree of cellular organization acquired by the tissue-infiltrating lymphocytes. Rheumatoid synovitis is associated with the formation of complex lymphoid microstructures, to the extent that the rheumatoid process induces the formation of T cell-B cell follicles with germinal center (GC) reactions in the synovium (1–3). These microstructures share many features with secondary lymphoid tissue, and the formation of GCs at an extranodal site can, therefore, be considered as an example of lymphoid neogenesis. The structural requirements permitting the generation of tertiary lymphoid tissue have not been examined. Also, it is not known which molecular pathways are used or which factors determine the type of lymphoid organization in individual patients.

A close relationship between inflammation and lymphoid organogenesis has been suggested by the finding that proinflammatory cytokines, such as members of the TNF superfamily, have a critical role in both processes (4, 5). Initially, it was found that mice deficient in lymphotoxin (LT) had no lymph nodes or Peyer's patches and failed to form GCs in the spleen (6, 7). Despite the absence of GCs, LT- $\alpha^{-/-}$  mice still produced high-affinity IgG1 responses, provided the mice were immunized with high doses of Ag (8). Gene targeting has been successfully used to implicate other molecules in the process of lymphoid organogenesis, including LT- $\beta$ , type I TNFR, and the LT- $\beta$ R (9–11). Mice with defects in these genes display different structural abnormalities and functional impairment of secondary lymphoid organs. In essence, signals transmitted by LT- $\alpha$ 1 $\beta$ 2 appear to be pivotal in the ontogeny of secondary lymphoid organs (12, 13).

More recently, studies of lymphoid organogenesis have focused on the contribution of chemokines that provide the cues to guide cell movement inside lymphoid organs (14, 15). Much progress has been made in understanding how the two major populations of lymphocytes are directed either to B cell or T cell zones and how chemokines control the movements of such cells during the development of Ag-specific immune responses. Mice homozygous for the spontaneous mutation, paucity of lymph node T cells (*plt*), are characterized by major abnormalities in T cell trafficking into lymph nodes and disturbances in the organization of T cell zones (16, 17). These mice lack expression of secondary lymphoid chemoattractant (SLC/CCL21) (18), which binds to CCR7. Defects in the movement of lymphocytes and DCs through the T cell areas of spleen, lymph nodes, and Peyer's patches are shared by *plt* and CCR7-deficient mice, establishing a critical role of this receptor-ligand pair in compartmental homing of T cells (19). Homeostatic trafficking of B cells into lymphoid tissue and B cell follicles appears to be critically controlled by B lymphocyte chemoattractant (BLC/CXCL13) (20, 21). The receptor for BLC/CXCL13,

Departments of \*Medicine and Immunology, <sup>†</sup>Laboratory Medicine and Pathology, <sup>‡</sup>Health Services Research, and <sup>§</sup>Orthopedic Surgery, Mayo Clinic, Rochester, MN 55905

Received for publication January 24, 2001. Accepted for publication May 9, 2001.

The costs of publication of this article were defrayed in part by the payment of page charges. This article must therefore be hereby marked *advertisement* in accordance with 18 U.S.C. Section 1734 solely to indicate this fact.

<sup>1</sup>This work was supported by grants from the National Institutes of Health (R01 AI44142, R01 AR42527, and R01 AR41974) and the Mayo Foundation.

<sup>2</sup>S.T. and A.B. contributed equally to this study.

<sup>3</sup>Address correspondence and reprint requests to Dr. Cornelia M. Weyand, Mayo Clinic, Guggenheim 401, 200 First Street SW, Rochester, MN 55905. E-mail address: weyand.cornelia@mayo.edu

<sup>4</sup>Abbreviations used in this paper: RA, rheumatoid arthritis; GC, germinal center; BLC, B lymphocyte chemoattractant; CD21L, CD21 long isoform; DC-CK1, dendritic cell-derived C-C chemokine 1; FDC, follicular DC; LT, lymphotoxin; MCP, macrophage chemoattractant protein; *plt*, paucity of lymph node T cells; SLC, secondary lymphoid chemoattractant.

CXCR5, is expressed on recirculating B cells; in *in vitro* chemotaxis assays, BLC/CXCL13 attracts B cells. In mice with a targeted inactivation of CXCR5, the normal development of Peyer's patches, inguinal lymph nodes, splenic follicles, and peripheral lymphocytes is disrupted, making the BLC/CXCL13-CXCR5 receptor-ligand pair critical in lymphoid tissue organization (15).

We studied a large cohort of patients with RA who presented with different phenotypes of lymphoid microarchitectures in the synovial lesions and examined whether cytokines and chemokines implicated in the genesis of secondary lymphoid organs are involved in the process of lymphoid neogenesis in RA. Analysis of the cellular elements in the synovium demonstrated that T cells, B cells, macrophages, and DCs were universally present in rheumatoid synovitis irrespective of the topographical organization of the infiltrate. In contrast, follicular DCs (FDCs) were limited to a subset of patients. Their presence perfectly correlated with the formation of secondary follicles and GCs. Multivariate regression analysis identified LT- $\beta$  and BLC/CXCL13 as independent critical variables in distinguishing patients with and without synovial GCs. These data suggest that seeding with FDCs or their precursors is the critical step in follicle formation in the synovium and occurs in some, but not all, patients. LT- $\alpha$ 1 $\beta$ 2 and BLC/CXCL13 may recruit or retain this highly specialized cell to extranodal tissue sites, thus determining the ultimate organization and function of tissue-invading lymphocytes in rheumatoid synovitis.

#### Materials and Methods

##### Study population

Synovial tissue was obtained from 64 patients with active RA who fulfilled the American College of Rheumatology 1987 revised criteria for RA and who underwent joint surgery. All patients provided informed consent. The study was approved by the Mayo Clinic Internal Review Board.

##### Histopathological evaluations

Hematoxylin sections of the synovial tissue samples were analyzed for the organizational structure of the inflammatory infiltrate with particular attention to the topographical arrangement of T cells, B cells, and macrophages. All analysis was performed by one hemopathologist (P.J.K.) who

was unaware of any clinical or laboratory findings. Tissue specimens were grouped according to the following criteria: 1) T cell-B cell aggregates with GCs, 2) T cell-B cell aggregates without GCs, or 3) diffuse infiltration of T cells and B cells and the absence of lymphoid organization. GCs within lymphoid aggregates were identified by standard histological criteria (22). These included well-circumscribed clusters of centrocytes and centroblasts with variable numbers of tingible body macrophages and mitotic figures within aggregates of small lymphocytes. In most cases, cells with the morphological features of FDCs were also associated with the centrocytes and centroblasts.

##### RT-PCR and cytokine semiquantification

Total RNA was extracted from synovial tissue specimens using a commercially available reagent (TRIzol; Invitrogen Life Technologies, Grand Island, NY). cDNA from synovial tissue specimens was analyzed for  $\beta$ -actin-specific sequences by semiquantitative PCR-ELISA and then adjusted to contain equal numbers. Adjusted cDNA was amplified by PCR for 30 cycles under nonsaturating conditions with cytokine-specific primers (Table I) in parallel with a standard containing a known number of cytokine sequences (23, 24). Each PCR amplification cycle consisted of denaturation at 94°C for 30 s, annealing at either 55°C ( $\beta$ -actin, BLC/CXCL13, LT- $\beta$ , MCP-1/CCL2, and DC-derived C-C chemokine (DC-CK1/CCL18)), 58°C (LT- $\alpha$ , and LT- $\beta$ R), or 60°C (SLC/CCL21) for 1 min, and polymerization at 72°C for 1 min with 10-min denaturation at 94°C at the start of the reaction and a final 10-min extension at 72°C. Amplified products were labeled with digoxigenin-11-dUTP (Roche Molecular Biochemicals, Indianapolis, IN) and then semiquantified in a liquid hybridization assay with biotinylated internal probes (Table I) using a commercially available PCR-ELISA kit (Roche Molecular Biochemicals). Labeled PCR products were hybridized for 2.5 h with 200 ng/ml probe at 42°C for  $\beta$ -actin, at 50°C for DC-CK1/CCL18 and macrophage chemoattractant protein 1 (MCP-1)/CCL2, and at 55°C for LT- $\alpha$ , LT- $\beta$ , LT- $\beta$ R, BLC/CXCL13, and SLC/CCL21. Hybrids were immobilized on streptavidin-coated microtiter plates and, after washing, were detected with a peroxidase-labeled anti-digoxigenin Ab. Plates were developed by a color reaction using 2,2'-azino-bis-(3-ethylthiazoline-6-sulfonic acid) (diammonium salt) substrate and quantified using a kinetic microplate reader (Molecular Devices, Sunnyvale, CA). The number of cytokine-specific sequences was determined by interpolation with a standard curve and was expressed as the number of cytokine sequences per  $1 \times 10^6$   $\beta$ -actin sequences. A ratio of one cytokine-specific sequence per  $1 \times 10^6$   $\beta$ -actin sequences was arbitrarily defined as 1 U.

cDNA was amplified using a specific primer set for the CR-2/CD21 long isoform (CD21L) selectively expressed by FDCs (Table I) (25). Amplified

Table I. Nucleotide sequences of PCR primers and biotinylated probes

Gene	Accession No.	Oligonucleotide Sequence
$\beta$ -actin	NM_001101	5' Primer, ATGGCCACGGCTGCTCCAGC 3' Primer, CATGGTGGTGCCGCCAGACAG Probe, TTCCTTCTGGGCATGGAGT
LT- $\alpha$	E01275	5' Primer, GCTGCTCACCTCATTGGAGA 3' Primer, GGTGGATAGCTGGTCTCCCT Probe, CCAGTGGCATCTACTTCGTCTAC
LT- $\beta$	L11015	5' Primer, ATCAGGGAGGACTGGTAACGGA 3' Primer, GAGGTAATAGAGCCGTCCTGC Probe, GAGGAGCCAGAAACAGATCTCAG
LT- $\beta$ R	NM_002342	5' Primer, GGTGCCTCCATATGCGTCGG 3' Primer, GGGGACGCAGTGGTTGTTAC Probe, TGCAGGGACCAGAAAAGGAATAC
BLC/CXCL13	AF044197	5' Primer, TCTCTGCTTCTCATGCTGCTGG 3' Primer, AGCTTGAGGGTCCACACACACA Probe, TCCCTAGACGCTTCATTGATCG
DC-CK1/CCL18	Y13710	5' Primer, GGTGTCATCCTCCTAACCAAG 3' Primer, GGAAAGGGGAAAGGATGATA Probe, CTTTTAAGAGTCCCCTCTGCTATG
MCP-1/CCL2	M24545	5' Primer, CAAGGGCTCGCTCAGCC 3' Primer, GCAATTTCCCAAGTCTCTG Probe, GAAGACTTGAACACTCACTCCAC
SLC/CCL21	AB002409	5' Primer, CCCAGGACCCAAGGCAGTGAT 3' Primer, TGTGACCGCTCAGTCTCTTGC Probe, CTCATCCCAGCTATCCTGTTC
CD21L	J03565	5' Primer, GTGGATTTACTTTGAAGGCCA 3' Primer, GGCATGTTTCTTCACACCG

products were analyzed by 2% agarose gel electrophoresis. PCR conditions were as described for amplification of products for PCR-ELISA. The annealing temperature for the primer set was 55°C.

### Antibodies

The following Abs were used for immunohistochemistry; mouse anti-human CD4 mAb (1:100; Dako, Carpinteria, CA), mouse anti-human CD20 mAb (1:100; Dako), goat anti-human BLC/BCA-1/SCYB13 polyclonal Ab (1:200; R&D Systems, Minneapolis, MN), mouse anti-human LT- $\beta$  mAb, B9.C9 (AC10) and B27.B2 (26, 27) (from J. L. Browning, Biogen, Cambridge, MA), mouse anti-human TNF- $\beta$  (LT- $\alpha$ ) mAb (R&D Systems), and mouse anti-human CXCR5 (BLR-1) mAb (R&D Systems). Secondary Ab used were peroxidase-labeled goat anti-mouse IgG (1:300; Kirkegaard & Perry Laboratories, Gaithersburg, MD) and biotinylated rabbit anti-goat Ig (1:300; Dako).

### Immunohistochemistry

Frozen synovial tissues embedded in OCT (Sakura Finetek USA, Torrance, CA) were cut into 5- $\mu$ m sections, mounted on slides (SuperFrost/Plus; Fisher Scientific, Pittsburgh, PA), and stored at -70°C. Before staining, the slides were fixed in acetone for 10 min, air dried, and fixed in 1% paraformaldehyde/EDTA (pH 7.2) for 3 min. Endogenous peroxidase was blocked with 0.3% H<sub>2</sub>O<sub>2</sub> in 0.1% sodium azide. Nonspecific binding was blocked for 15 min with 5% normal goat serum (Invitrogen Life Technologies) or porcine serum (Sigma, St. Louis, MO), dependent on the species of secondary Ab.

For double-staining with LT- $\alpha$ 1 $\beta$ 2 and CD20 Abs, the EnVision<sup>+</sup> system (Dako) was used. Sections were fixed as above, blocked with 5% swine serum for 15 min, and incubated with mouse anti-human LT- $\alpha$ 1 $\beta$ 2 mAb (1:200) for 30 min at room temperature. Thoroughly washed sections were treated for 30 min with the EnVision<sup>+</sup> reaction system and developed with 3,3'-diaminobenzidine tetrahydrochloride. The 3,3'-diaminobenzidine tetrahydrochloride-stained slides were washed in tap water. Nonspecific binding was blocked for 15 min with 5% goat serum, and sections were stained with mouse anti-human CD20 mAb (1:100; Dako) for 60 min at room temperature. After incubation with biotinylated rabbit anti-mouse Ig Ab (1:300; Dako), the slides were incubated with the VectaStain avidin-

biotin complex-alkaline phosphatase kit (Vector Laboratories, Burlingame, CA) for 30 min and then developed with a Vector Red substrate kit (Vector Laboratories) for 3 min. Slides were counterstained with hematoxylin for 5 s and permanently mounted in Cytoseal-60 (Stephens Scientific, Riverdale, NJ). Negative controls were stained with secondary Ab without the primary Ab.

### Statistical analysis

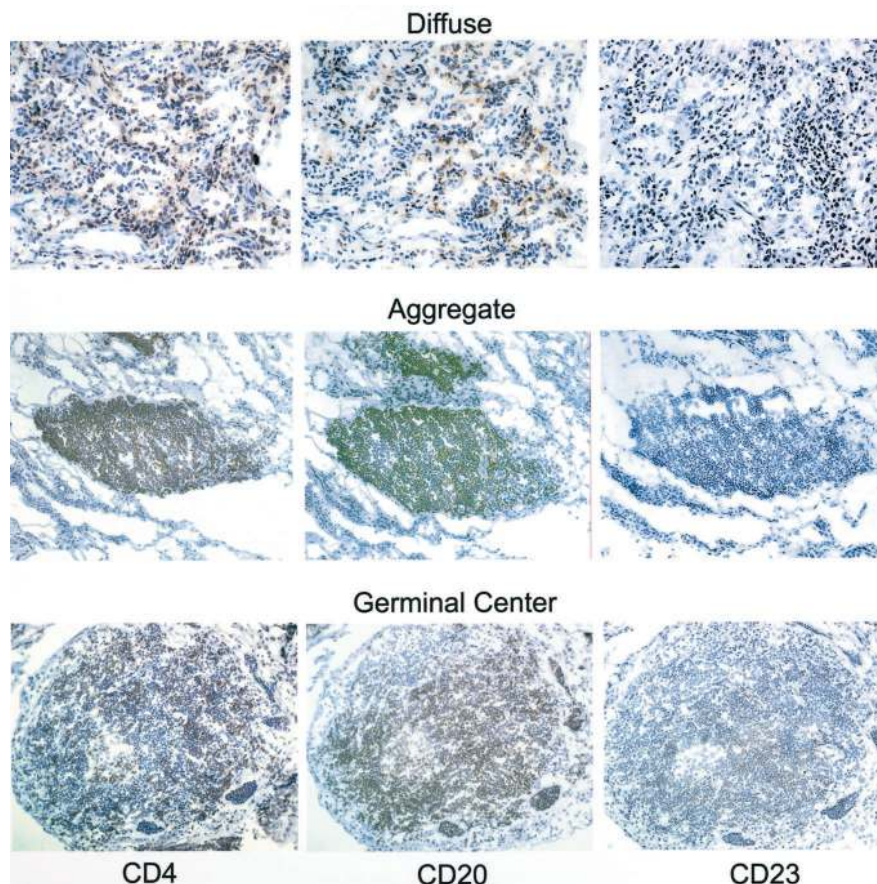
Synovial tissue types were compared by nonparametric testing using SigmaStat software (SPSS, Chicago, IL) for the relative level of cytokine transcripts as determined by RT-PCR. Continuous variables (relative cytokine transcript concentrations) were analyzed by recursive partitioning to define optimal cutoffs. Logistic models were then used to identify variables that correlated with an increased likelihood of GC formation. Analysis was done using SAS statistical software (SAS Institute, Cary, NC).

## Results

### Synovial lymphoid microstructures

Synovial tissues from 64 RA patients were obtained at the time of synovectomy or joint replacement surgery and were analyzed for the topographical organization of the inflammatory infiltrate. The arrangements of tissue-invading cells in rheumatoid synovitis were diverse, but three distinct patterns could be distinguished (Fig. 1). In 36 tissues (56.3%), T cells, B cells, macrophages, and DCs were arranged as diffuse infiltrates without specific microstructures. In tissues from the other 28 patients, B cells formed clusters, generally combined with T cells. Such cell clusters were either organized as secondary follicles with GC reactions (15 tissues or 23.4%) or presented as T cell-B cell aggregates lacking GCs (13 tissues or 20.3%). These two patterns were mutually exclusive; lymphoid aggregates with and without GCs were not found in parallel in the same tissues. GC<sup>+</sup> follicles were characterized by B cell proliferation, loss of central IgD-expressing B cells, and the

**FIGURE 1.** Pattern of lymphoid organizations in rheumatoid synovitis. Serial sections of synovial tissues were stained with anti-CD4 (left), anti-CD20 (center), or anti-CD23 mAb (right). In a subset of patients ( $n = 36$ ), T cells and B cells were diffusely distributed throughout the tissue. Other patients ( $n = 13$ ) formed T cell-B cell aggregates lacking FDCs and GC reactions. In the third subset of patients ( $n = 15$ ), T cell-B cell follicles with typical GC reactions in the center were identified. Original magnification,  $\times 400$  (diffuse),  $\times 200$  (aggregate and GC).



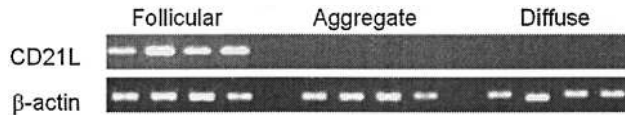


**FIGURE 2.** Expression of CD21L, a specific marker for FDCs, is limited to synovial tissues with GC<sup>+</sup> follicles. cDNA was generated from all synovial biopsies and amplified with primers specific for CD21L and for  $\beta$ -actin. Four representative examples for each histological pattern of RA synovitis are shown. CD21L-specific sequences were exclusively expressed in follicular tissues with GC reactions.

presence of FDC networks. B cells in T cell-B cell aggregates without GCs did not actively proliferate and FDC networks were not detectable (3). Both types of tissues with clustering of B cells and T cells contained plasma cells that tended to accumulate under the synovial lining layer. CD83<sup>+</sup> DCs were present in all variants of rheumatoid synovitis.

#### FDCs are restricted to a subset of RA tissues

FDCs are an essential cellular component of B cell follicles in secondary lymphoid tissues. To assess whether all synovial tissue samples contained these cells, immunohistochemical stains for CD23 were performed (Fig. 1). To avoid sampling artifacts, PCR for a constitutive marker of FDCs, CD21L (25), was performed in parallel (Fig. 2). Both approaches yielded the same result. FDCs were found in 15 of 64 tissues (23.4%) analyzed. In all biopsies with a positive signal for CD21L mRNA, follicles with GC reactions were present. In all tissues lacking GC<sup>+</sup> follicles, CD21L was undetectable. In particular, tissues with T cell-B cell aggregates without GCs lacked FDCs, indicating that these structures are different from primary follicles. This finding demonstrated that the lymphoid neogenesis in the rheumatoid synovium fundamentally differed from secondary lymphoid organs. The exclusive finding of GCs but no primary follicles suggested that the lymphoid neogenesis in the synovium is strictly dependent on an Ag recognition event, in distinction to normal lymph nodes. The selective

presence of FDCs also indicated that these cells are not a regular component of the synovial tissue.

#### Correlation of tissue cytokine pattern and lymphoid microstructures

To identify cytokines and chemokines contributing to the formation of synovial GCs, LT- $\alpha$  and LT- $\beta$  transcripts were semiquantified after adjustment for the number of  $\beta$ -actin transcripts. As shown in Fig. 3, tissues with GC<sup>+</sup> follicles contained significantly more LT- $\alpha$  and LT- $\beta$  mRNA than the two other tissue types. Both cytokines were expressed at distinctly low levels in tissues with aggregates or diffuse synovitis. In biopsies with GC<sup>+</sup> synovitis, the median for LT- $\alpha$  was 182 U; LT- $\beta$ -specific sequences were present with a median of 441 U. In synovial tissue samples with T cell-B cell aggregates, the median values for LT- $\alpha$  and LT- $\beta$  were 42 and 35 U, respectively. Tissues with diffuse synovitis were essentially negative for LT- $\alpha$ -specific sequences and had low LT- $\beta$  mRNA.

LT- $\alpha$ 1 $\beta$ 2 binds to the LT- $\beta$ R. Functional activity of LT- $\beta$ , therefore, depends on the availability of LT- $\beta$ R<sup>+</sup> cells. Expression of LT- $\beta$ R in the synovial microenvironment was analyzed by PCR. All tissue extracts contained mRNA for LT- $\beta$ R. There was a trend for GC tissues to have higher numbers of LT- $\beta$ R transcripts, but this was not statistically significant.

#### Correlation of tissue chemokine profiles and lymphoid microstructures

BLC/CXCL13 and SLC/CCL21 are critical players in the formation of secondary lymphoid tissues (28–30) and are expressed in chronic inflammatory lesions. BLC/CXCL13 mRNA was detected in synovial tissue extracts at varying levels depending on the lymphoid microstructure encountered in the biopsy (Fig. 4). The highest quantities of BLC/CXCL13 mRNA were detected in GC-positive synovium, 15- to 30-fold higher than in tissues with T cell-B cell aggregates ( $p = 0.001$ ) or diffuse lymphocytic infiltrates ( $p < 0.001$ ). There was a trend for BLC/CXCL13 to be higher in aggregate-positive tissues than in diffuse tissues (median of 159 vs 89

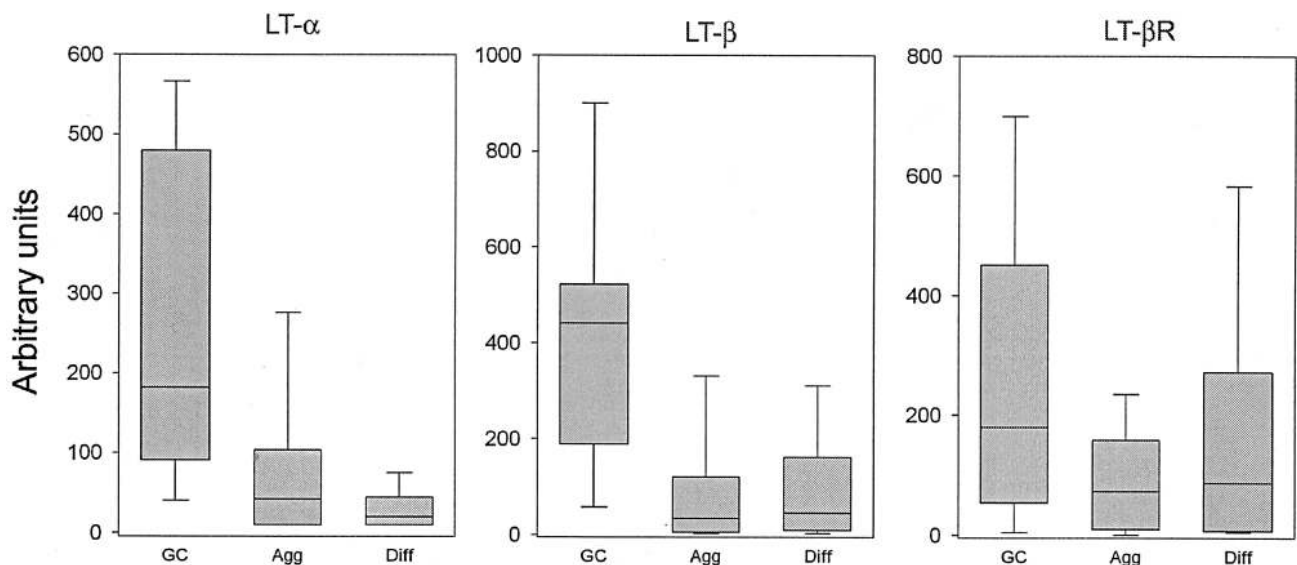
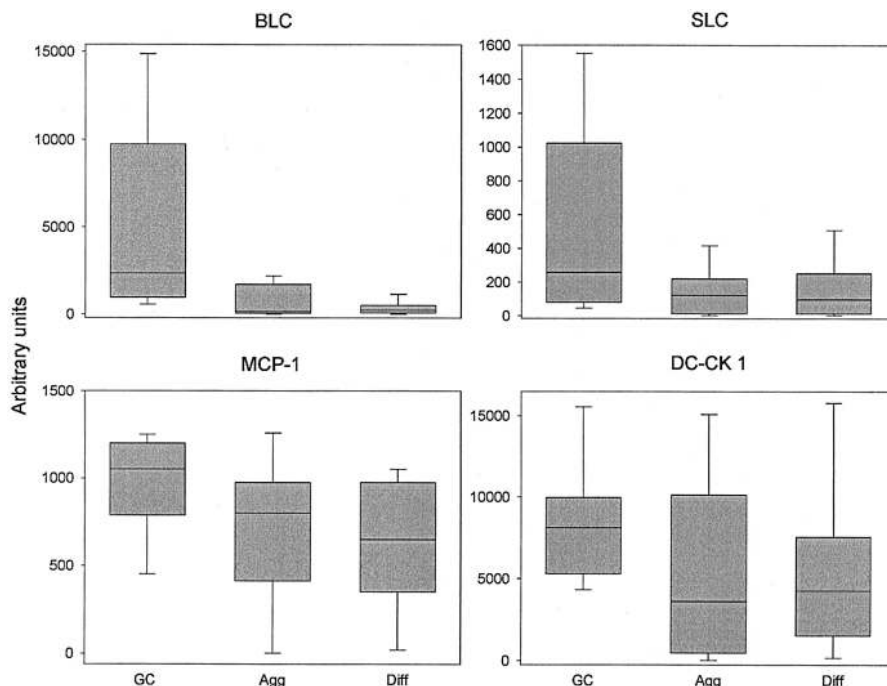


**FIGURE 3.** In situ transcription of LT- $\alpha$  and LT- $\beta$  correlates with the pattern of lymphoid microstructure formed in RA synovitis. Tissue samples were stratified according to the pattern of synovitis. LT- $\alpha$ , LT- $\beta$ , and LT- $\beta$ R transcripts in tissue extracts were semiquantified by RT-PCR and liquid oligonucleotide hybridization. Results of the measurements are given as arbitrary units after normalization for  $\beta$ -actin. Box plots show medians, 25th and 75th percentiles as boxes, and 10th and 90th percentiles as whiskers. Levels of LT- $\alpha$  and LT- $\beta$  transcripts were significantly higher in tissues with GC<sup>+</sup> follicles (GC) compared with tissues with T cell-B cell aggregates lacking GCs (Agg) or tissues with diffuse synovitis (Diff). There was no statistically significant difference in LT- $\beta$ R expression. GC-negative aggregates and diffuse synovitis did not differ for any of the three markers.

**FIGURE 4.** BLC/CXCL13 and SLC/CCL21 but not MCP-1/CCL2 and DC-CK1/CCL18 are associated with GC formation. Production of mRNA for the chemokines BLC/CXCL13, SLC/CCL21, MCP-1/CCL2, and DC-CK1/CCL18 was measured in all synovial tissues. The highest amount of BLC/CXCL13- and SLC/CCL21-specific transcripts were detected in tissue samples with GC reactions (GC). BLC/CXCL13 and SLC/CCL21 were low in tissues with GC-negative T cell-B cell aggregates (Agg) and in diffuse (Diff) synovitis. Similar quantities of MCP-1/CCL2 and DC-CK1/CCL18 transcripts were found in all three types of rheumatoid synovitis. Results are given as box blots as described in the legend to Fig. 3.



U) that did not reach statistical significance ( $p = 0.262$ ). Essentially all samples with secondary follicles contained BLC/CXCL13 mRNA in severalfold higher quantities than the average GC-negative cases. However, the aggregate as well as the diffuse synovitis group included four and three samples, respectively, with BLC/CXCL13 results above 1000 U, indicating that BLC/CXCL13 can be transcribed in the absence of lymphoid follicles.

Synovial tissue biopsies containing GCs were also characterized by increased transcription of SLC/CCL21. The differences between the tissue types, however, were not as marked as for BLC/CXCL13. The median units in follicular synovium were 2-fold higher than in T cell-B cell aggregate tissues (258 vs 124 U,  $p = 0.059$ ) and significantly higher than in diffuse synovitis ( $p = 0.013$ ). No difference in SLC/CCL21 mRNA was observed between diffuse and aggregate synovitis ( $p = 0.726$ ). Again, high production of SLC/CCL21 mRNA was seen in 2 of the 36 biopsies with diffuse infiltrates. There was no correlation between SLC/CCL21 and BLC/CXCL13 in the study cohort. In particular, GC-negative cases with expression of either chemokine did not coincide.

To rule out the possibility that the overrepresentation of BLC/CXCL13 and SLC/CCL21 in the GC<sup>+</sup> follicles was simply a reflection of increased inflammatory activity, two additional chemokines, DC-CK1/CCL18 and MCP-1/CCL2 were analyzed. Results are given in Fig. 4. All tissue extracts contained transcripts for DC-CK1/CCL18 and MCP-1/CCL2. Tissues with secondary follicles had the highest values for DC-CK1/CCL18, but they were not significantly different from those in the aggregate-positive or diffuse cases. MCP-1/CCL2 levels were comparable in all synovitis subsets. Median values varied between 700 U in the diffuse samples and 1050 U in the tissues with follicles.

In summary, we found preferential expression of SLC/CCL21 and BLC/CXCL13, two chemokines implicated in regulating trafficking of T cells and B cells in lymphoid tissues, in synovial tissue specimens containing GCs.

#### Predicting GC<sup>+</sup> synovitis by logistic regression modeling

Several variables distinguished tissues with and without GC formation, including expression of LT- $\alpha$ , LT- $\beta$ , BLC/CXCL13, and

SLC/CCL21. In an attempt to estimate the relative contribution of these parameters to the process of synovial GC formation, data were analyzed using logistic models. Because lymphoid aggregate and diffuse tissues did not differ for any of the variables (Figs. 3 and 4), GC<sup>+</sup> tissues were compared with the remaining tissues. None of the variables had a Gaussian distribution. Each continuous variable was, therefore, transformed into a discrete variable by recursive partitioning. Logistic regression analysis was performed to determine whether the dichotomized variables correlated with GC formation. In the univariate analysis, high mRNA of all seven markers were predictive of synovial GCs (data not shown). However, tissue concentrations of LT- $\beta$  and BLC/CXCL13 transcripts were by far the most powerful predictors of GC reactions in the synovial lesion. The probability of encountering synovial GCs was 31-fold higher if LT- $\beta$  transcripts were present at units above 315. Similarly, tissue expression of BLC/CXCL13 sequences at >1800 U increased the probability of GC formation by a factor of 31.

To explore whether the different cytokines were dependent or independent variables in the molecular pathways generating synovial GCs, multivariate analysis was performed. As shown in Table II, LT- $\beta$  and BLC/CXCL13 were independent predictors of GC

Table II. Multivariate logistic regression modeling for synovial GC formation

Variable	Cutoff Point <sup>a</sup>	Odds Ratio (95% CI) <sup>b</sup>	$p$
LT- $\beta$	315	15.45 (2.72–87.59)	0.002
BLC/CXCL13	1800	14.03 (2.22–88.58)	0.005
Adjusting for the two variables above:			
SLC/CCL21	550	14.17 (1.30–159.60)	0.03 <sup>c</sup>
LT- $\alpha$	110	3.56 (0.49–25.69)	0.209
MCP-1/CCL2	875	1.60 (0.26–9.96)	0.617
DC-CK1/CCL18	3840	— (0.00–999.00)	0.954

<sup>a</sup> Optimal cutoff points for cytokine mRNA quantities were identified by recursive partitioning. Multivariate logistic regression models were developed using the stepwise approach.

<sup>b</sup> CI, Confidence interval.

<sup>c</sup> In bootstrap variable selection, this variable did not meet the requirements for entry into the multivariate logistic regression model (43).

formation. Significance for SLC/CCL21 was lost after bootstrapping was performed for validation of the variables in the model (43). None of the other parameters continued to be significant after correction for LT- $\beta$  and BLC/CXCL13 measurements. The model that best predicted GC formation was based on the following two assumptions, reflecting the independent contribution of BLC/CXCL13 and LT- $\beta$ : 1) patients with low BLC/CXCL13 (<1800 U) and low LT- $\beta$  (<315 U, defined by the recursive partitioning) have no GCs, and 2) patients with high BLC/CXCL13 and/or LT- $\beta$  have GCs. The model had a sensitivity of 86.7% and a specificity of 87.8% to correctly predict GC formation (Table III). The positive predictive value was 68.4%, i.e., only 11 of the 17 tissues predicted were true GC formers. Six of the 17 tissues fulfilled the cytokine criteria but did not form GCs, indicating that the mere presence of high LT- $\beta$  and/or BLC/CXCL13 transcripts was not sufficient to guarantee follicle formation and that other variables, e.g., cytokines not included in our analysis, may play a role. The negative predictive value of the model was excellent (95.6%, Table III), suggesting that GC formation does not occur if both of these mediators are below a certain threshold. The alternative model, requiring high concentrations of either cytokine, lacked sensitivity.

#### *The cellular origin of LT- $\beta$ and BLC/CXCL13 in rheumatoid synovitis*

The strong predictive value of either LT- $\beta$  or BLC/CXCL13 in identifying tissues with GC reactions raised the question of which cell types supplied these two factors in the synovial microenvironment. Immunohistochemical staining was used to detect membrane-bound LT- $\beta$  in rheumatoid synovitis. Staining of peripheral blood B cells served as positive controls; 80–85% of all circulating CD20<sup>+</sup> B cells expressed LT- $\beta$ . In secondary lymphoid tissues, such as tonsils, weak staining could be localized to few cells in secondary follicles. More prominent staining results were obtained in synovial tissue sections. Sections from biopsies with diffuse synovitis or T cell-B cell aggregates were negative. Synovial tissue B cell follicles with GC reactions yielded a positive signal for LT- $\beta$  (Fig. 5). A subset of the CD20<sup>+</sup> B cells in the follicular centers stained with anti-LT- $\beta$  Ab. A subpopulation of B cells in the mantle zone was also positive for surface LT- $\beta$  protein. No morphological or topographical characteristics were found distinguishing LT- $\beta$ <sup>-</sup> and LT- $\beta$ <sup>+</sup> B cells. LT- $\beta$  staining was not restricted to CD20<sup>+</sup> cells. Follicular structures also included lymphoid non-B cells staining positive. These cells expressed CD4, identifying them as CD4<sup>+</sup> T cells. The majority of T and B cells in the tissue, however, did not stain for LT- $\beta$ . LT- $\beta$  positivity of CD20<sup>+</sup> and CD20<sup>null</sup> cells was associated with follicles and was not encountered in interfollicular regions.

Production of BLC/CXCL13 in the spleen and lymph nodes has been attributed to stromal cells, most likely FDCs. Immunohisto-

chemical analysis of synovial sections revealed intense staining with anti-BLC/CXCL13 Ab within the GCs. The staining pattern was compatible with FDCs expressing BLC/CXCL13 (Fig. 6). Frequently, the cytoplasm of follicular center B cells also stained with the Ab, whereas mantle zone cells were consistently negative. BLC/CXCL13 production in the synovial tissue was not restricted to follicular centers. In patients with or without GC<sup>+</sup> follicles, BLC/CXCL13 protein was detected on endothelial cells of capillaries and small arterioles. Yet another cell population contributed to BLC/CXCL13 production in the synovial lesions; intense staining was consistently found on synovial lining cells. In addition, isolated synoviocytes, dispersed throughout the tissue, expressed BLC/CXCL13 protein.

## Discussion

Lymphoid follicles with GC reactions are a characteristic of synovial lesions in RA, yet these sophisticated microstructures are generated in only a subset of patients. The current study incorporated a large series of synovial tissue biopsies to define molecular components of the process of lymphoid neogenesis in extranodal sites and to identify parameters predicting GC formation in individual patients. Distinct clustering of T cells and B cells was found in 44% of all synovial tissues, approximately one-half of them had GC reactions. Our study documents that the emergence of GCs in the synovium is not dependent on a single variable but requires the concerted action of several independent cellular responses, in particular, the production of LT- $\beta$  and BLC/CXCL13. Interestingly, LT- $\beta$  and BLC/CXCL13 were independently regulated and could, in part, substitute for each other. LT- $\alpha$ 1 $\beta$ 2 originated from lymphoid cells, mainly B cells, whereas BLC/CXCL13 was predominantly supplied by ancillary cells of the synovial membrane. The ability of synovial tissue cells to participate in BLC/CXCL13 production is obviously a factor guiding lymphoid neogenesis to this tissue site. Recruitment of FDCs or their precursors was identified as the ultimate determinant in regulating lymphoid organization in the joint.

Emergence of GC<sup>+</sup> follicles in extranodal sites is considered as a critical step in the generation of autoimmune process (31). It is not unique for RA and has also been observed in other chronic inflammatory syndromes such as hepatitis C infection, Sjögren's syndrome, *Helicobacter pylori*-associated gastric mucosa-associated lymphoid tissue, and Hashimoto's thyroiditis (32–35), but usually in only a subset of cases. It is not known why only some patients can generate these highly structured lymphoid organizations. Evidence for a critical role of host-response factors in determining whether or not GCs are formed in the synovium comes from prospective monitoring of multiple successive tissue lesions in RA patients. We have found that the pattern of lymphoid arrangement in the joint lesions is stable over time in individual patients and that samples harvested from multiple different joints will contain the same type of synovitis (S. Takemura, P. J. Kurtin, J. J. Guronzy, and C. M. Weyand, manuscript in preparation). An additional possible explanation is that Ags driving rheumatoid synovitis are diverse and that the particular topography of the lymphoid infiltrates is a reflection of the type of Ag encountered in the synovial membrane. Precedence for this model comes from the observation that lymphadenitis is characterized by preferential activation of submicroenvironments in lymph nodes, depending on the Ag that elicits the immune response. For example, EBV-induced lymphadenitis is known to lead to profound activation of paracortical T cell zones, whereas bacterial infections with streptococci can be expected to produce follicular lymphoid hyperplasia (36).

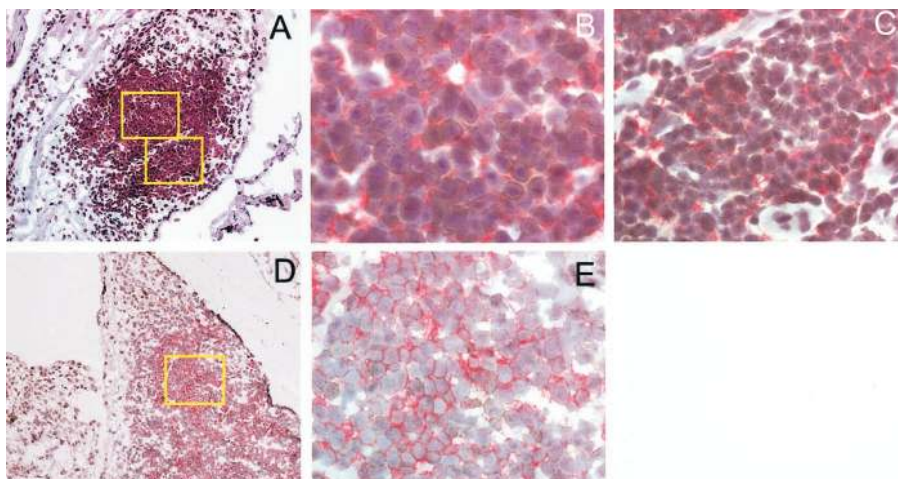
Results of the current study indicate that the molecules implicated in the development of secondary lymphoid organs are also

Table III. Prediction of GC formation assuming independent contribution of tissue LT- $\beta$  and tissue BLC/CXCL13

GC Present	GC Predicted <sup>a</sup>		Total
	No	Yes	
No	43	6	49
Yes	2	13	15
Total	45	19	64

<sup>a</sup> In this model, GCs were predicted to form if either BLC/CXCL13 or LT- $\beta$  exceeded the cutoff defined by recursive partitioning. (BLC/CXCL13 > 1800 U; LT- $\beta$  > 315 U). Positive predictive value of the model, 68.4%; negative predictive value of the model, 95.6%.

**FIGURE 5.** Cellular origin of LT- $\beta$ . Two-color immunohistochemistry of frozen tissue sections was performed to identify cells expressing LT- $\alpha 1\beta 2$  (brown). B cells were immunostained with anti-CD20 mAb (red). Representative sections from two tissues at original magnifications of  $\times 200$  (A and D) and  $\times 1000$  (B, C, and E) are shown. Three different cell populations, all with lymphoid morphology, reacted with anti-LT- $\beta$  mAb. LT- $\beta^+$  B cells were found in the follicular centers of GCs (B). Mantle zones contained a small subpopulation of LT- $\beta^+$ CD20 $^+$  cells (C). LT- $\beta$  was also expressed on CD20 $^{\text{null}}$  cells, mostly localized in GCs (E). Staining with anti-CD4 identified these cells as T cells (data not shown).



critically involved when tertiary lymphoid structures are formed. Elegant studies in gene-targeted mice have suggested that aberrant expression of LT- $\alpha$  may be sufficient to induce the generation of lymph node-like structures in nonlymphoid tissues (5). Induction of chemokines and adhesion molecules on endothelial cells and, thus, regulation of cell recruitment have been suggested as an underlying mechanism through which LT- $\alpha$  could determine lymphoid neogenesis (37). A recent study provided evidence for an ultimately critical position of BLC/CXCL13 in the process of lymphoid neogenesis (38). In transgenic mice expressing BLC/CXCL13 in the pancreatic islets, lymph node-like structures emerged with B cell and T cell zones, high endothelial venules, and production of SLC/CCL21. Studies in *H. pylori*-induced mucosa-associated lymphoid tissue have shown high-level expression of BLC/CXCL13 in all lymphoid aggregates (39). From these studies, it could be concluded that the isolated presence of LT- $\alpha$  or BLC/CXCL13 would be sufficient to initiate the process of extranodal lymphoid neogenesis. Human studies have the limitation that the process of GC induction and establishment has to be retrospectively analyzed. However, in this study, multivariate logistic regression analysis allowed for the identification and hierarchical modeling of markers associated with GC $^+$  synovial follicles.

In the univariate analysis, all seven cytokines/chemokines correlated with synovial GC reactions, provided they were present at high concentrations. However, the multivariate analysis demonstrated that only two markers emerged as independent determinants, LT- $\beta$  and BLC/CXCL13. All other molecules were dependent variables. In particular, LT- $\alpha$  that is found in the soluble LT- $\alpha 3$  cytokine, as well as in the LT- $\alpha 1\beta 2$  molecule, was a dependent variable, suggesting that LT- $\alpha 1\beta 2$ , and not LT- $\alpha 3$ , is im-

portant in GC formation in the synovial tissue. Although high transcription of BLC/CXCL13 in the tissue increased the likelihood of finding GCs, the isolated expression of BLC/CXCL13-specific sequences was not sufficient to predict GC formation. Several patients had high BLC/CXCL13 mRNA in the synovium but failed to form typical follicles, indicating that the relationship between BLC/CXCL13 expression and structuring of lymphoid infiltrates is more complex in rheumatoid synovitis than in the murine models. Modeling of the data suggested that BLC/CXCL13 and LT- $\beta$  concentrations were critical but could substitute for each other to some degree, raising the interesting question how the chemokine BLC/CXCL13 and the membrane-integrated cytokine LT- $\alpha 1\beta 2$  could compensate for each other in lymphoid neogenesis. The negative predictive value of this model was excellent, indicating that the formation/maintenance of synovial follicles is essentially impossible if the concentrations of both mediators are below a critical threshold. The positive predictive value was moderate, suggesting that high concentrations of either mediator was not always sufficient to guarantee the process of GC formation. In particular, there were patients with high BLC/CXCL13 and high LT- $\beta$  who did not form GCs, suggesting that additional factors are required besides aberrant expression of LT- $\beta$  and BLC/CXCL13. One such factor could be the availability of FDCs. The absence of FDCs, documented by immunohistochemical staining as well as PCR for CD21L, in tissue samples free of GCs was surprising and established that the synovial membrane differs fundamentally from lymphoid organs. Not a single example was found of a primary follicle, i.e., the presence of FDCs without a fully developed GC reaction. FDCs participated in GC reactions whenever they were present. Whether patients with the ability to form synovial GCs are

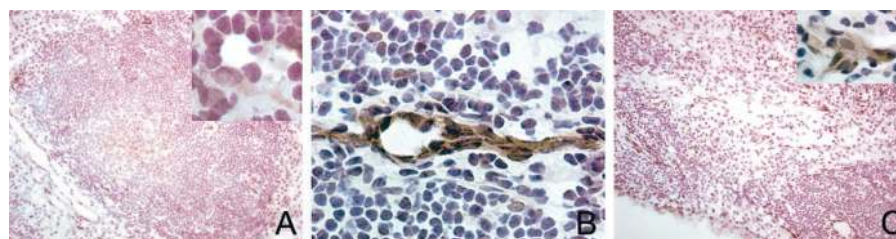


**FIGURE 6.** Cellular origin of BLC/CXCL13. BLC/CXCL13 protein was immunolocalized in synovial tissue by histochemistry. Frozen sections of synovial biopsies were stained with anti-BLC/CXCL13 mAb (brown). BLC/CXCL13 was consistently produced in follicular centers where it was detected on the surface of FDCs (A) but also on some centroblasts; mantle zones were negative for BLC/CXCL13. Endothelial cells lining small arterioles and capillaries stained for BLC/CXCL13 (B), as did synovial fibroblasts in the lining and the sublining tissue (C). Endothelial staining and BLC/CXCL13 production by synoviocytes was irrespective of whether the tissue contained GCs or not. Insets in A and C show staining of individual cells. Original magnification,  $\times 200$  (A and C),  $\times 400$  (B), and  $\times 1000$  (insets).



carriers of FDCs at that tissue site or recruit the precursor or mature FDCs to that site needs to be explored. The ontogeny of FDCs is not completely understood. A recent publication has suggested that synovial fibroblasts may share functional characteristics with FDCs, including the ability to cluster B cells on their surface (40, 41). We have seen BLC/CXCL13 expression in isolated synovial fibroblasts (Fig. 5), but we have not been able to induce CD21L expression or the production of BLC/CXCL13 in synovial fibroblast lines, two features that would be suggestive of a relationship between synoviocytes and FDCs (data not shown). The perfect correlation between FDC presence and GC reaction emphasizes the critical contribution of Ag recognition events in the process of lymphoid neogenesis in RA. The total lack of primary follicles suggests that Ag-specific T cells and B cells precede FDCs and may actually be necessary for the recruitment, differentiation, or survival of FDCs in the synovial microenvironment.

Our finding that the B cell is an origin of LT- $\beta$  is in-line with previous studies, providing evidence of a critical role of B cells and LT- $\beta$  in the process of secondary lymphoid tissue development. LT- $\beta$  is expressed on the vast majority of circulating B cells (data not shown). However, in the tissue, only a subset of B cells in the mantle zone and a small proportion of B cells in the GCs express LT- $\beta$ . T cell-B cell aggregates, although rich in B cells, contained very few LT- $\beta$  transcripts. The reason that B cells appear to lose LT- $\beta$  expression as they infiltrate into the tissue and that only selected B cells continue to produce LT- $\beta$  once in the tissue lesion requires additional studies. At least two different mechanisms have been identified to up-regulate membrane LT- $\alpha$ 1 $\beta$ 2 expression on B cells. One mechanism implicates BLC/CXCL13 in inducing B cell surface expression of LT- $\alpha$ 1 $\beta$ 2; the second mechanism is BLC/CXCL13 independent (15). In our studies, BLC/CXCL13 and LT- $\beta$  did not correlate, and the multivariate modeling demonstrated their relative independence in the induction of GCs.

Identifying B cells as a cellular origin of LT- $\beta$ , critically involved in the decision process of how the lymphocytic infiltrate in RA joints is organized, emphasizes that B cells have multiple functions in rheumatoid synovitis extending far beyond a simple role of releasing autoantibodies (42). However, T cells participating in follicles also expressed LT- $\beta$ , raising the question whether additional cell populations contribute to the decision process to establish a GC reaction in this extranodal site.

BLC/CXCL13 derived from several different cellular sources. Endothelial cells lining capillaries and small arterioles were by far the most frequent cell types that stained with anti-BLC Abs. Endothelial cells are generally not considered a major source of this chemokine. Therefore, it cannot be excluded that the BLC detected was passively adsorbed. However, BLC/CXCL13-positive endothelial cells were present in synovial tissues of all types, including tissues with no GC reaction and no FDCs, suggesting that endothelial cells may indeed be producer cells. BLC/CXCL13 was consistently expressed in GCs, in-line with the interpretation that FDCs are an important source for this chemokine. Nevertheless, BLC/CXCL13 expression was not restricted to FDCs and was even found in synoviocytes. This observation emphasizes that the tissue structure hosting the immune reaction, in this case, the synovial membrane, may be directly involved in directing the organization of infiltrating lymphocytes. Heterotypic signaling between the diverse cell types within rheumatoid lesions may ultimately provide an explanation why the synovial membrane is chosen as a site for extranodal lymphoid neogenesis.

This study has several clinical implications. It is important to realize that the rheumatoid lesion not only has the ability to facilitate tissue destruction but can also function like a lymph node.

The complexity of lymphoid microstructures amplifies Ag-specific responses, and much lower concentrations of Ag are required for Ag-specific reactions to occur (31). One of the interesting questions is whether immune responses in the synovial membrane are restricted to Ags present in the local environment or whether Ag trapping and enrichment could also become relevant for Ags not primarily involved in the disease process. If that were the case, the joint could provide the infrastructure to support immune responses against nonarthritogenic Ags. This could be of particular relevance for patients producing rheumatoid factor, an autoantibody binding to the Fc portion of IgG. It is known that synovial fluid is rich in immunocomplexes, possibly providing a wide spectrum of Ags to be handled in the tertiary lymphoid tissue structures of the joint. Another important lesson from the current study is that the sharing of molecular mechanisms in the formation of secondary and tertiary lymphoid organizations may limit the use of BLC/CXCL13 and LT- $\beta$  as targets for immunosuppressive therapy in RA. Obviously, BLC/CXCL13- or LT- $\beta$ -directed therapy would pose the risk of also destroying lymphoid follicles in lymph nodes, spleen, and Peyer's patches. The interesting finding that FDCs are not a constitutive cell population of the synovial membrane should initiate studies into the processes of FDC recruitment to sites of tertiary lymphoid tissue formation. Inhibition of that process could provide an elegant approach to suppress rheumatoid synovitis.

## Acknowledgments

We thank Jeff Browning at Biogen for his generous gift of the mAb against LT- $\beta$ . We also thank Tammy J. Dahl and James W. Fulbright for assistance with manuscript preparation and graphics.

## References

- Young, C. L., T. C. Adamson III, J. H. Vaughan, and R. I. Fox. 1984. Immunohistologic characterization of synovial membrane lymphocytes in rheumatoid arthritis. *Arthritis Rheum.* 27:32.
- Schroder, A. E., A. Greiner, C. Seyfert, and C. Berek. 1996. Differentiation of B cells in the nonlymphoid tissue of the synovial membrane of patients with rheumatoid arthritis. *Proc. Natl. Acad. Sci. USA* 93:221.
- Wagner, U. G., P. J. Kurtin, A. Wahner, M. Brackertz, D. J. Berry, J. J. Goronzy, and C. M. Weyand. 1998. The role of CD8<sup>+</sup> CD40L<sup>+</sup> T cells in the formation of germinal centers in rheumatoid synovitis. *J. Immunol.* 161:6390.
- Ruddle, N. H. 1999. Lymphoid neo-organogenesis: lymphotoxin's role in inflammation and development. *Immunol. Res.* 19:119.
- Kratz, A., A. Campos-Neto, M. S. Hanson, and N. H. Ruddle. 1996. Chronic inflammation caused by lymphotoxin is lymphoid neogenesis. *J. Exp. Med.* 183:1461.
- De Togni, P., J. Goellner, N. H. Ruddle, P. R. Streeter, A. Fick, S. Mariathasan, S. C. Smith, R. Carlson, L. P. Shornick, and J. Strauss-Schoenberger. 1994. Abnormal development of peripheral lymphoid organs in mice deficient in lymphotoxin. *Science* 264:703.
- Fu, Y. X., H. Molina, M. Matsumoto, G. Huang, J. Min, and D. D. Chaplin. 1997. Lymphotoxin- $\alpha$  (LT $\alpha$ ) supports development of splenic follicular structure that is required for IgG responses. *J. Exp. Med.* 185:2111.
- Matsumoto, M., S. F. Lo, C. J. Carruthers, J. Min, S. Mariathasan, G. Huang, D. R. Plas, S. M. Martin, R. S. Geha, M. H. Nahm, and D. D. Chaplin. 1996. Affinity maturation without germinal centres in lymphotoxin- $\alpha$ -deficient mice. *Nature* 382:462.
- Matsumoto, M., Y. X. Fu, H. Molina, and D. D. Chaplin. 1997. Lymphotoxin- $\alpha$ -deficient and TNF receptor-I-deficient mice define developmental and functional characteristics of germinal centers. *Immunol. Rev.* 156:137.
- Koni, P. A., R. Sacca, P. Lawton, J. L. Browning, N. H. Ruddle, and R. A. Flavell. 1997. Distinct roles in lymphoid organogenesis for lymphotoxins  $\alpha$  and  $\beta$  revealed in lymphotoxin  $\beta$ -deficient mice. *Immunity* 6:491.
- Futterer, A., K. Mink, A. Luz, M.H., and K. Pfeffer. 1998. The lymphotoxin  $\beta$  receptor controls organogenesis and affinity maturation in peripheral lymphoid tissues. *Immunity* 9:59.
- Matsumoto, M., Y. X. Fu, H. Molina, G. Huang, J. Kim, D. A. Thomas, M. H. Nahm, and D. D. Chaplin. 1997. Distinct roles of lymphotoxin  $\alpha$  and the type I tumor necrosis factor (TNF) receptor in the establishment of follicular dendritic cells from non-bone marrow-derived cells. *J. Exp. Med.* 186:1997.
- Cyster, J. G. 1999. Chemokines and cell migration in secondary lymphoid organs. *Science* 286:2098.
- Cyster, J. G., V. N. Ngo, E. H. Eklund, M. D. Gunn, J. D. Sedgwick, and K. M. Ansel. 1999. Chemokines and B-cell homing to follicles. *Curr. Top. Microbiol. Immunol.* 246:87.
- Ansel, K. M., V. N. Ngo, P. L. Hyman, S. A. Luther, R. Forster, J. D. Sedgwick, J. L. Browning, M. Lipp, and J. G. Cyster. 2000. A chemokine-driven positive feedback loop organizes lymphoid follicles. *Nature* 406:309.

16. Gunn, M. D., S. Kyuwa, C. Tam, T. Kakiuchi, A. Matsuzawa, L. T. Williams, and H. Nakano. 1999. Mice lacking expression of secondary lymphoid organ chemokine have defects in lymphocyte homing and dendritic cell localization. *J. Exp. Med.* 189:451.
17. Nakano, H., S. Mori, H. Yonekawa, H. Nariuchi, A. Matsuzawa, and T. Kakiuchi. 1998. A novel mutant gene involved in T-lymphocyte-specific homing into peripheral lymphoid organs on mouse chromosome 4. *Blood* 91:2886.
18. Vassileva, G., H. Soto, A. Zlotnik, H. Nakano, T. Kakiuchi, J. A. Hedrick, and S. A. Lira. 1999. The reduced expression of 6Ckine in the *plt* mouse results from the deletion of one of two 6Ckine genes. *J. Exp. Med.* 190:1183.
19. Forster, R., A. Schubel, D. Breitfeld, E. Kremmer, I. Renner-Muller, E. Wolf, and M. Lipp. 1999. CCR7 coordinates the primary immune response by establishing functional microenvironments in secondary lymphoid organs. *Cell* 99:23.
20. Forster, R., T. Emrich, E. Kremmer, and M. Lipp. 1994. Expression of the G-protein-coupled receptor BLR1 defines mature, recirculating B cells and a subset of T-helper memory cells. *Blood* 84:830.
21. Forster, R., A. E. Mattis, E. Kremmer, E. Wolf, G. Brem, and M. Lipp. 1996. A putative chemokine receptor, BLR1, directs B cell migration to defined lymphoid organs and specific anatomic compartments of the spleen. *Cell* 87:1037.
22. van der Valk, P., and C. Meijer. 1987. The histology of reactive lymph nodes. *Am. J. Surg. Pathol.* 11:866.
23. Brack, A., H. L. Rittner, B. R. Younge, C. Kaltschmidt, C. M. Weyand, and J. J. Goronzy. 1997. Glucocorticoid-mediated repression of cytokine gene transcription in human arteritis-SCID chimeras. *J. Clin. Invest.* 99:2842.
24. Klimiuk, P. A., J. J. Goronzy, J. Bjornsson, R. D. Beckenbaugh, and C. M. Weyand. 1997. Tissue cytokine patterns distinguish variants of rheumatoid synovitis. *Am. J. Pathol.* 151:1311.
25. Liu, Y. J., J. Xu, O. de Bouteiller, C. L. Parham, G. Grouard, O. Djossou, B. de Saint-Vis, S. Lebecque, J. Banchereau, and K. W. Moore. 1997. Follicular dendritic cells specifically express the long CR2/CD21 isoform. *J. Exp. Med.* 185:165.
26. Browning, J. L., I. Dougas, A. Ngam-ek, P. R. Bourdon, B. N. Ehrenfels, K. Miatkowski, M. Zafari, A. M. Yampaglia, P. Lawton, W. Meier, et al. 1995. Characterization of surface lymphotoxin forms: use of specific monoclonal antibodies and soluble receptors. *J. Immunol.* 154:33.
27. Cannella, B., I. D. Sizing, C. D. Benjamin, J. L. Browning, and C. S. Raine. 1997. Antibodies to lymphotoxin  $\alpha$  (LT  $\alpha$ ) and LT  $\beta$  recognize different glial cell types in the central nervous system. *J. Neuroimmunol.* 78:172.
28. Hjelmstrom, P., J. Fjell, T. Nakagawa, R. Sacca, C. A. Cuff, and N. H. Ruddle. 2000. Lymphoid tissue homing chemokines are expressed in chronic inflammation. *Am. J. Pathol.* 156:1133.
29. Cyster, J. G. 2000. Leukocyte migration: scent of the T zone. *Curr. Biol.* 10:R30.
30. Ngo, V. N., H. Korner, M. D. Gunn, K. N. Schmidt, D. S. Riminton, M. D. Cooper, J. L. Browning, J. D. Sedgwick, and J. G. Cyster. 1999. Lymphotoxin  $\alpha/\beta$  and tumor necrosis factor are required for stromal cell expression of homing chemokines in B and T cell areas of the spleen. *J. Exp. Med.* 189:403.
31. Fehr, T., C. Lopez-Macias, B. Odermatt, R. M. Torres, D. B. Schubart, T. L. O'Keefe, P. Matthias, H. Hengartner, and R. M. Zinkernagel. 2000. Correlation of anti-viral B cell responses and splenic morphology with expression of B cell-specific molecules. *Int. Immunol.* 12:1275.
32. Banerjee, S. K., A. P. Weston, M. N. Zoubine, D. R. Campbell, and R. Chierian. 2000. Expression of cdc2 and cyclin B1 in *Helicobacter pylori*-associated gastric MALT and MALT lymphoma: relationship to cell death, proliferation, and transformation. *Am. J. Pathol.* 156:217.
33. Freni, M. A., D. Artuso, G. Gerken, C. Spanti, T. Marafioti, N. Alessi, A. Spadaro, A. Ajello, and O. Ferrau. 1995. Focal lymphocytic aggregates in chronic hepatitis C: occurrence, immunohistochemical characterization, and relation to markers of autoimmunity. *Hepatology* 22:389.
34. Lennert, K., and U. Schmid. 1983. Preliminary, early lymphoma, and manifest lymphoma in immunosialadenitis (Sjogren's syndrome): a model of lymphomagenesis. *Haematol. Bluttransfus* 28:418.
35. Imal, Y., and M. Yamakawa. 1996. Morphology, function and pathology of follicular dendritic cells. *Pathol. Int.* 46:807.
36. Schnitzer, B. 1995. Reactive lymphoid hyperplasia. In *Surgical Pathology of the Lymph Nodes and Related Organs*, 2nd Ed. E. S. Jaffe, ed. Saunders, Philadelphia, p. 98.
37. Cuff, C. A., J. Schwartz, C. M. Bergman, K. S. Russell, J. R. Bender, and N. H. Ruddle. 1998. Lymphotoxin  $\alpha 3$  induces chemokines and adhesion molecules: insight into the role of LT $\alpha$  in inflammation and lymphoid organ development. *J. Immunol.* 161:6853.
38. Luther, S. A., T. Lopez, W. Bai, D. Hanahan, and J. G. Cyster. 2000. BLC expression in pancreatic islets causes B cell recruitment and lymphotoxin-dependent lymphoid neogenesis. *Immunity* 12:471.
39. Mazzucchelli, L., A. Blaser, A. Kappeler, P. Scharli, J. Laissue, M. Baggiolini, and M. Uguccioni. 1999. BCA-1 is highly expressed in *Helicobacter pylori*-induced mucosa-associated lymphoid tissue and gastric lymphoma. *J. Clin. Invest.* 104:49.
40. Lindhout, E., M. van Eijk, M. van Pel, J. Lindeman, H. J. Dinant, and C. de Groot. 1999. Fibroblast-like synoviocytes from rheumatoid arthritis patients have intrinsic properties of follicular dendritic cells. *J. Immunol.* 162:5949.
41. Bofill, M., A. N. Akbar, and P. L. Amlot. 2000. Follicular dendritic cells share a membrane-bound protein with fibroblasts. *J. Pathol.* 191:217.
42. Weyand, C. M., J. J. Goronzy, S. Takemura, and P. J. Kurtin. 2000. T cell-B cell interactions in rheumatoid arthritis. *Arthritis Res.* 2:457.
43. Sauerbrei, W., and M. Schumacher. 1992. A bootstrap resampling procedure for model building: application to the Cox regression model. *Stat. Med.* 11:2093.